Construction and Building Materials 352 (2022) 129052

Contents lists available at ScienceDirect

Construction and Building Materials

journal homepage: www.elsevier.com/locate/conbuildmat

Sound absorption, structure and mechanical behavior of konjac glucomannan-based aerogels with addition of gelatin and wheat straw

Yixin Wang [a,c], Hui Zhu [b,*], Wenyao Tu [c], Yuehong Su [a], Fatang Jiang [a,c], Saffa Riffat [a]

[a] Department of Architecture and Built Environment, Faculty of Engineering, University of Nottingham, NG7 2RD, UK
[b] Department of Mechanical, Materials and Manufacturing Engineering, Faculty of Engineering, University of Nottingham, NG7 2RD, UK
[c] Glyn O. Phillips Hydrocolloid Research Centre at HBUT, National "111" Center for Cellular Regulation and Molecular Pharmaceutics, School of Food and Biological Engineering, Hubei University of Technology, Wuhan 430068, China

ARTICLE INFO

Keywords:
Konjac glucomannan-based aerogel
Gelatin
Wheat straw
Sound absorption
Pore structure
Mechanical property
Mechanical model

ABSTRACT

Environment-friendly konjac glucomannan (KGM)-based aerogels with addition of gelatin and wheat straw are produced by freeze-drying method to have promising sound absorption performance, thermal stability and mechanical property. Results show that gelatin addition can significantly improve sound absorption performance at medium and high frequencies, as well as mechanical strength, because of the positive effect on increase of small open pores. Appropriate little addition of wheat straw can improve the sound absorption property due to the dissipation effect of sound energy by the unique multi-cavity structure. Better sound absorption performance is achieved than melamine foam, while the best result is obtained with a noise reduction coefficient of 0.38, and the coefficient reaches 0.88 at 4500 Hz. Wheat straw addition leads to strength reduction firstly but enhancement when the addition is more than 1.00%, where fine wheat straw bars form nest structures for strengthening. For potential loading capacity evaluation, a mechanical model is proposed and confirmed to be effective in predicting compressive stress – strain relationship of KGM-based aerogels with consideration of gelatin and wheat straw addition.

1. Introduction

Noise pollution has been drawing increasing attention with urban and technological developments, especially since people rely more on cars in their daily life [1]. Currently, a range of acoustic insulation or absorption materials are used in the construction industry to reduce the impact of noise on people's life. In accordance with the difference in material structure, sound absorption materials can be classified to have porous, resonant [2] and peculiar geometry [3] structures. Among them, porous materials are most commonly used in building field, such as organic fibers (natural and plant fibers), inorganic fibers (glass fibers), polymeric, inorganic, metallic foams and so on. A large number of porous structures on the surface and inside contribute to the good sound absorption performance of porous materials. When sound waves pass through the material, a part of sound energy is reflected. The rest enters porous material and is converted into heat energy by the vibration or friction of material. Many studies have been carried out to develop and investigate the sound absorption performance of difference porous materials [4–7]. As porous cement-based materials are acknowledged to be useful in pavement sound absorption, Yoon et al. [8] successfully improved the performance by enhancing the pore structure with addition of natural fibers and aluminum powder into cement. Wang and Du [9] developed recycled aggregate crumb rubber concrete with recycled aggregate and rubber particles from waste tire mixture and rubber pad. The authors found this material could be qualifying in sound absorption application and proposed to use it in building partition walls. Inorganic porous materials have also been widely investigated in many studies, which were focused on the preparation by use of fly ash, coal gangue, blast furnace slag and other industrial solid wastes. In the research of Wu et al. [10], ammonium hydrogen carbonate was used as pore former to reveal the effect of pore former and other process parameters on the apparent porosity, pore size and sound absorption property of the developed ceramsites.

As a kind of typical porous material, an aerogel is proposed by Kistler [11] for the first time. This kind of synthetic porous ultralight material is derived from a gel, in which the liquid component of the gel is replaced

* Corresponding author.
E-mail addresses: celiax@126.com (Y. Wang), hui.zhu@nottingham.ac.uk (H. Zhu), twy1073981169@163.com (W. Tu), yuehong.su@nottingham.ac.uk (Y. Su), jiangft@mail.hbut.edu.cn (F. Jiang), saffa.riffat@nottingham.ac.uk (S. Riffat).

https://doi.org/10.1016/j.conbuildmat.2022.129052
Received 2 May 2022; Received in revised form 24 August 2022; Accepted 1 September 2022
Available online 11 September 2022

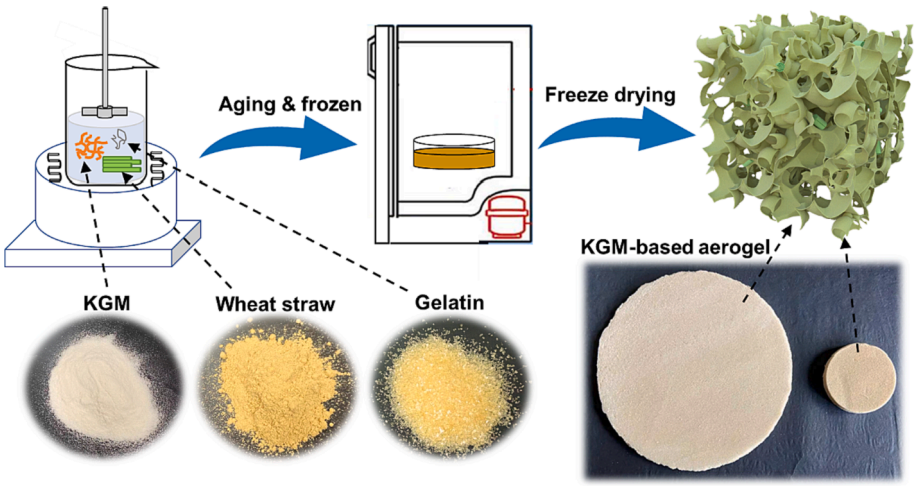

Fig. 1. Schematic procedure for preparing KGM-based aerogels.

by gas and a porous solid with extremely low density, large interior surface area is formed [12]. Since then, various aerogels have been invented with wide uses because of these superior characteristics. However, most traditional aerogels and those that are currently being studied, such as polyethylene, polyurethane foam and silica aerogels are made from unsustainable inorganic products or petrochemical-based materials. Instead, in recent years, biodegradable biomass-based aerogels have been attracting great interest and providing a superior alternative to conventional aerogels [13–17]. With abundant sources, polysaccharides including cellulose [18,19], chitosan [15,20], pectin [16], starch [21], alginate [22] and agar [23] are adopted to prepare composite aerogels. Some researchers have explored the possibility to use biomass-based aerogels as sound absorption materials. As reported by Lu et al. [24], the lignocellulose aerogels were prepared via different freezing–thawing treatments. In this study, the sound absorption coefficient can reach 0.877 and 0.78.2 at 1000 Hz and 2000 Hz, respectively. Pu et al. [25] adopted gelatin and semi-liquefied waste bamboo to produce functional aerogels with good sound absorption performance. To reuse the natural plant waste, Do et al. [26] proposed to use pineapple waste as raw materials to combine with polyvinyl alcohol to prepare aerogels for sound absorption. These biomass materials are abundantly resourced, low-cost, environmentally friendly, and are the key to producing environmentally friendly building materials.

As a promising polysaccharide, Konjac glucomannan (KGM) was reported having the potential to be a skeletal material in gel due to its macromolecular chain structures [27,28], and KGM-based aerogels exhibit good three-dimensional network structures [27,29–31]. Due to the unique light-weight and pore structure, KGM-based aerogels have the possibility to be a promising sound absorption material after a preliminary test by Wang et al. [32]. Based on the knowledge obtained from the previous research, the control of porous structures and pore sizes are essential in preparation of KGM-based aerogel as a sound absorption material, so gelatin and wheat straw are used in this study. Gelatin is a collagen peptide derived from the skin [33,34], bone and cartilage of animals, and is widely used as a bionic scaffold in tissue culture engineering because of its biocompatible and porous properties [35]. Wheat straw is a kind of agricultural wastes, main components of which are cellulose, hemicellulose and lignin [36]. Currently, the common way to dispose wheat straw is by burning, which causes serious air pollution to the environment. In this study, by adopting wheat straw as a raw material to prepare KGM-based aerogel, a new approach to utilize it and improve its economic value is explored.

The purpose of this study is to propose a new porous biomass-based aerogel for sound absorption. KGM-based aerogels with addition of gelatin and wheat straw are produced via sol–gel process and then obtained after freeze-drying. The physical and chemical properties including microstructure, sound absorption properties, thermal stability and mechanical properties are investigated. With the appropriate addition of gelatin and wheat straw, KGM-based aerogels show good compatibility and improved sound absorption property. Based on the compressive testing results, a mechanical model is proposed and used to predict the stress – strain behavior of KGM-based aerogels with considering the effects of gelatin and wheat straw additions. Along with the testing results, the interactions among KGM, gelatin and wheat straw are revealed, and the property enhancement mechanism is explored and discussed. This study has a guiding value for the material design, selection, and practical application aspects of KGM-based aerogels.

2. Materials and methods

2.1. Materials

KGM (Mw 911.5 KDa) was supplied by Hubei Konson Konjac Gum Co., ltd (China). Gelatin (Mw 245.2 KDa) was provided by Sinopharm Chemical Reagent Co., ltd. (China). The dried wheat straw was obtained from a local farm. After washing, drying, cutting and sieving process, the wheat straw powder was sieved through a 160-mesh sieve, the pore size of which is 0.096 mm (GB/T 6003.1–2012).

2.2. Preparation of KGM-based aerogels

KGM-based aerogels were produced through the sol–gel process and freeze-drying method based on previous researches [29,37] and patents [38]. A diagram is presented in Fig. 1 showing the preparation process of producing KGM-based aerogels. Gelatin (0–1.50%, w/v) was first dissolved in double-distilled water at 60 °C. After gelatin was dissolved completely, KGM (1.00%, w/v) with or without wheat straw (0–2.00%, w/v) was slowly added under constant stirring at 600 rpm, and the temperature was increased to 95 °C. After the mixture stirring for 1 h, KGM-based mixtures were obtained. After the aging process at 4 °C, the samples were immediately frozen in a freezer (LGT2325, German-Swiss) at −15 °C for 10 h. The frozen specimens were dried in a freeze dryer (FD-1A-50, Boyikang, China) at −55 °C under a vacuum of 1 Pa for approximately 24 h. To simplify the description of KGM-based aerogels, all samples were coded in the form of K0G0WS0. K, G, WS represents KGM, gelatin and wheat straw, respectively, and the number after K, G and WS indicates the weight volume percent of original biomass solution.

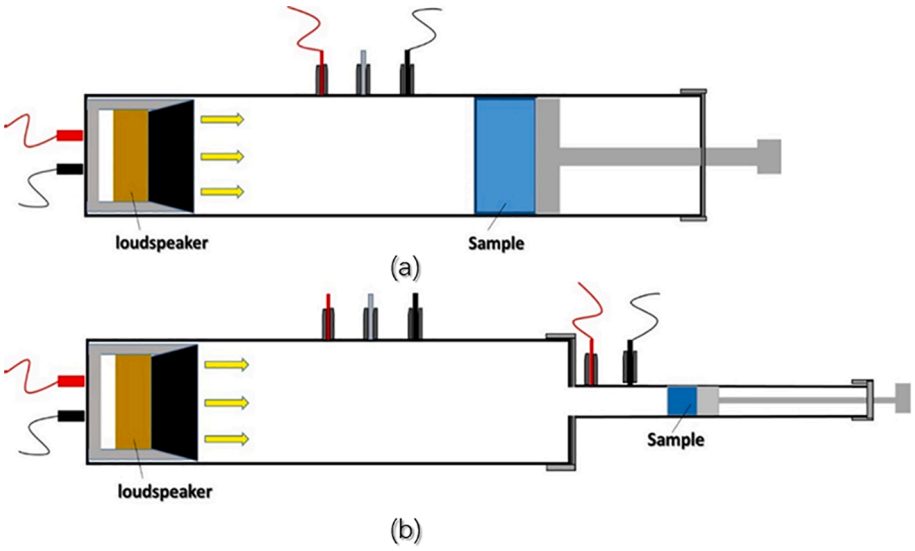

Fig. 2. Principle diagram of impedance tube for measurement of sound absorption coefficient at frequencies (a) from 50 to 1000 Hz and (b) from 500 to 6300 Hz.

2.3. Characterization methods

2.3.1. Microstructure observation and pore size distribution

Microstructure was observed with scanning electron microscopy (JSM6390LV, JEOL, Tokyo). Before all the tests, aerogels were cut and coated with gold particles. The pore size distribution was counted and analyzed by Image Pro Plus software. To reduce uncertainty, three representative SEM images of each aerogel were selected from three repeated samples for the observation. The width of pore diameter classes for number count is 10 μm.

2.3.2. Porosity measurement

To measure the porosity, the aerogel sample was soaked in ethanol in a container, then put in a vacuum oven, and vacuumized until no bubble coming out. The porosity was calculated by the following equation:

$$\text{Porosity}\ (\%) = \frac{\text{Weight of ethanol in the aerogel}}{\text{Total weight of aeroegl and ethanol}} = \frac{m_1 - m_2 - m}{m_1 - m_2} \quad (1)$$

where m is weight of the aerogel sample; m_1 is the total weight of the aerogel sample, ethanol and the container; m_2 is the weight of the remaining ethanol and the container after the aerogel sample was taken out.

2.3.3. Sound absorption coefficient measurement

The sound absorption coefficients at different frequencies were tested with zero air gap on the Impedance Tube AWA6122A (Hangzhou Aihua Instruments, China) at room temperature, the principle diagram of which is given in Fig. 2. Before tests, aerogel samples were cut into two different sizes: diameter of 30 mm, height of 10 mm for tests from 500 to 6300 Hz and diameter of 96 mm, height of 10 mm for tests from 50 to 1000 Hz. To ensure the testing precision, the gap between the interior surface of impedance tube and the sample perimeter was sealed with petroleum jelly after mounting the samples on the backing plate. For each aerogel material, three samples were tested. From the testing results, the noise reduction coefficient (NRC) value is defined as the average value of the individual sound absorption coefficients of specimen at 125, 250, 500, 1000, 2000 and 4000 Hz.

2.3.4. Mechanical property analysis

The mechanical properties of KGM-based aerogels were tested on a Texture analyzer (TA.XT Plus, Stable Micro Systems, Surrey, UK) equipped with a 5 kg load cell and a discoidal probe P/36R through

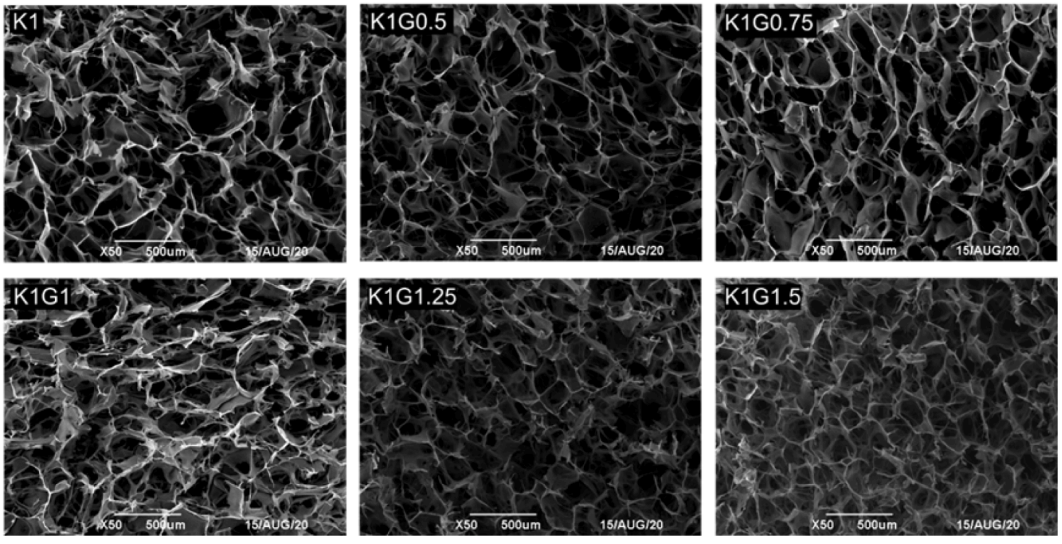

Fig. 3. SEM observation of KGM and KGM/gelatin aerogels.

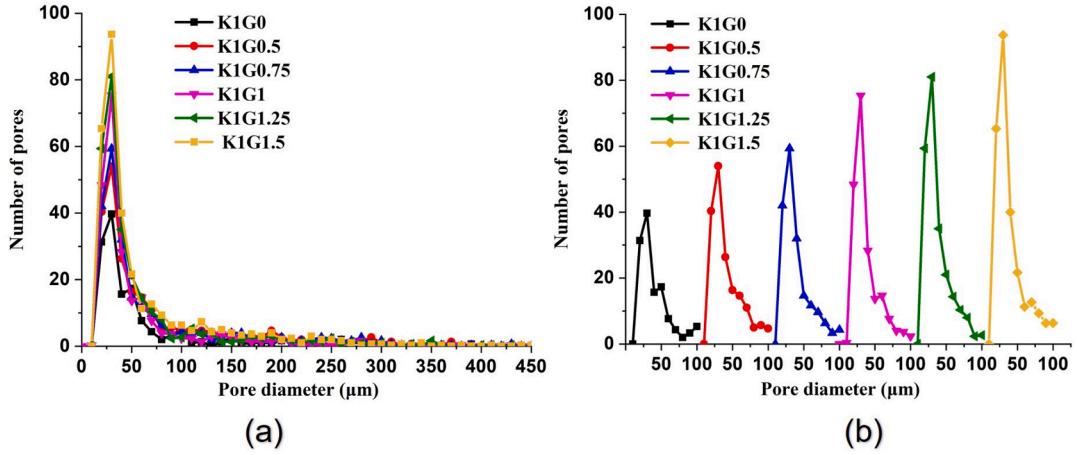

Fig. 4. Size distribution (a: 0–450 μm; b: 0–100 μm) of KGM/gelatin aerogels pores with different gelatin concentration. The width of the pore diameter classes for number count is 10 μm.

single compressive tests. The testing compression rate and ratio were 0.5 mm/*sec* and 45%, respectively. All the compressive tests were repeated with three samples of each aerogel material.

2.3.5. *Fourier transform infrared spectroscopy*

To analyze the chemical groups of raw materials and KGM-based aerogels and to test whether new chemical bonds were created among different raw materials, the developed aerogels were tested by a Fourier transform infrared spectroscopy (FTIR) spectrometer (VERTEX 70, Bruker Co., ltd Germany) with attenuated total reflection in the range of 4000–650 cm^{-1}. Before tests, all samples were dried for 48 h in a dryer. Data were collected in 32 scans at a resolution of 4 cm^{-1}.

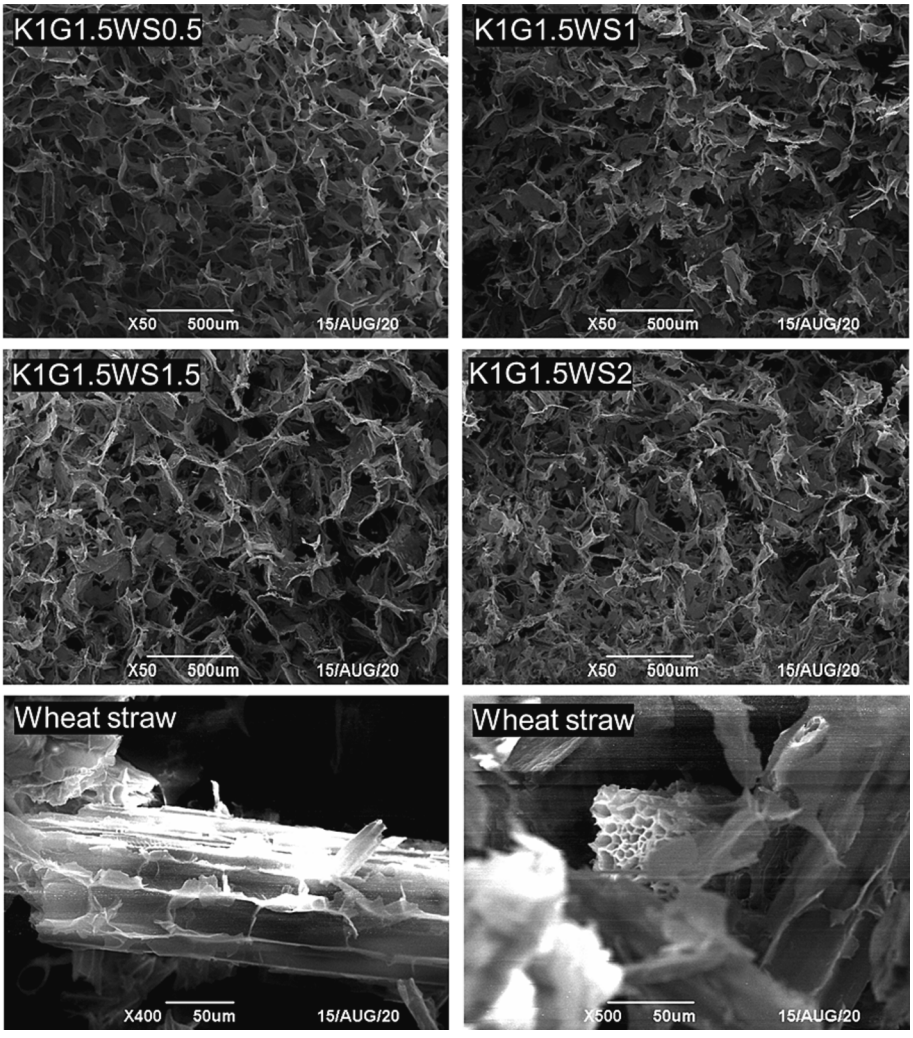

Fig. 5. SEM observation of KGM/gelatin/wheat straw aerogels.

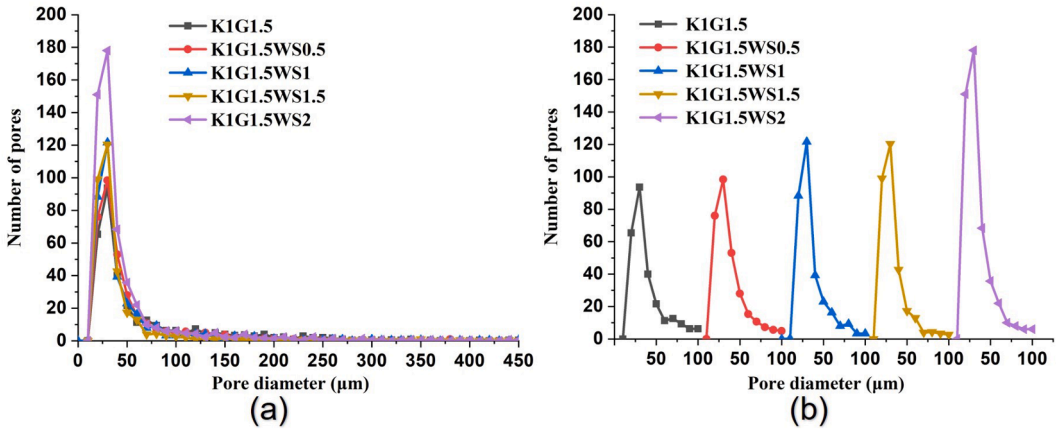

Fig. 6. Distribution of pore sizes (a) 0–450 μm and (b) 0–100 μm in KGM/gelatin/wheat straw aerogels with different wheat straw concentration. The width of the pore diameter classes for number count is 10 μm.

2.3.6. Thermogravimetric analysis

To identify the thermal stability of the developed KGM-based aerogels, thermogravimetric analysis (TGA) of the developed aerogels was characterized by a Thermogravimetric analyzer (Netzsch TG 209, Selb, Germany). After being pulverized, samples were heated from 25 °C to 600 °C with a heating rate of 20 °C/min in N_2 atmosphere and weight loss curves were recorded reflecting the thermostability of samples.

3. Results and discussion

3.1. Impact of gelatin and wheat straw on the microstructure of KGM-based aerogels

As given in Fig. 3, pure KGM aerogel shows a relatively spherical porous structure, formed by the water ice crystals sublimate during the freeze-drying process [39]. When adding and increasing the gelatin contents in pure KGM aerogels, the pore sizes of KGM-based aerogels are gradually decreased, and aerogel pore walls are thickened because of the increase of the total solid concentrations. In addition, pore structures of KGM/gelatin aerogels are interconnected with one another and present as open pores when gelatin is added. To further investigate the effect of gelatin content on aerogel pore structure, the pore size distribution of KGM/gelatin aerogels was statistically analyzed. As presented in Fig. 4 (a and b), the pore sizes of all KGM/gelatin aerogels mainly range from 1 to 100 μm. With gelatin content increases from 0.50% to 1.50% (w/v), the total pore numbers in aerogel with pore sizes of 0–50 μm are gradually increased, which is consistent with the observation from SEM images. With more gelatin addition, more small size hole cavities were formed. Gelatin is always used to provide intermediate structural support in composite constituents, meanwhile it can also act as the porogenic agent [40]. Compared with K1G0, gelatin addition of 0.50%, 0.75%, 1.00%, 1.25% and 1.50% can increase the number of pores with sizes of 0–50 μm by 31.73%, 42.31%, 59.62%, 88.78% and 112.18%, respectively. The numbers of small size pore of K1G1.25 and K1G1.5 are more than that of other KGM/gelatin aerogels. This may result from that the increasing amount of gelatin has an influence on the growth space of ice crystals, leading to the occurrence of more small pores. In addition, the increase of total solid concentration also leads to the reduction of pore channel sizes.

Fig. 5 shows SEM micrographs of KGM/gelatin/wheat straw aerogels with different wheat straw contents. After the addition of wheat straw, the aerogel pores become smaller and more complex from polygons into irregular shapes. The reason is that wheat straw addition may increase the resistance against the growth from KGM/gelatin mixture to ice crystals [41] and cause shape changes of ice crystal during the freezing process, which could affect the pore size distribution, the shape and the connectivity of the porous network [42]. As supported by the aerogel pore size distribution results (Fig. 6 a and b), wheat straw can also provide many micron-scale pores due to its multi-cavity structure as shown in Fig. 5. By analyzing the pore size distribution of KGM/gelatin/wheat straw aerogels, the peak number appears at pore diameter of 20–30 μm. There is a significant increase of peak value when wheat straw addition reaches 1.00% or 2.00%. The reason is that wheat straw with multi-cavity structure is randomly hugged in KGM/gelatin pore wall, displaying an open-cell geometry and contributing to the appearance of small size pores.

From the investigation of the pore structure of KGM-based aerogels, it can be concluded that the addition of gelatin could lead to the increase in number and proportion of small open pores because of the increased total solid concentration. While the addition of wheat straw could further benefit the appearance of small open pores and make the pore structure more complex due to the increased resistance against the growth from KGM/gelatin mixture to ice crystals and the unique multi-cavity structure of wheat straw.

3.2. Sound absorption property of KGM-based aerogels

The comparison of sound absorption performance among KGM-based aerogels with different material compositions is presented by Fig. 7, in which each curve is made of the sound absorption coefficient at different frequencies from 125 to 6300 Hz. Each material was tested with three samples, and the average values and error bars are used and presented. The possible reason for the measurement uncertainty may be the slight structure inhomogeneity of prepared samples and the imprecision in sample cutting. However, it can be found in Fig. 7 that the measurement errors do not have a significant influence on the general variation trend and the result analysis. As shown in Fig. 7 (a), with the separate addition of gelatin and wheat straw, significant difference of sound absorption coefficient is observed. Compared with K1WS3, the sound absorption performance of KGM/gelatin aerogels has a significantly improvement. The significant enhancement of sound absorption performance in high frequency range is correlated well with the homogeneous bulk density and structure of KGM/gelatin aerogels. Referring to the previous research [29], it was found that wheat straw subsidence can be easily observed in KGM/wheat straw mixtures. Due to this phenomenon, the upper part of K1WS3 has many large size pores while lots of wheat straw powder gathers at the bottom. As a result, the lower layer has higher density compared with the upper layer. The inhomogeneous density and pore structure may lead to the poor sound absorption performance. Different from KGM/wheat straw aerogels, the pores inside KGM/gelatin aerogels are hierarchically maze-like and distributed evenly. As presented in Fig. 3, there are a large number of

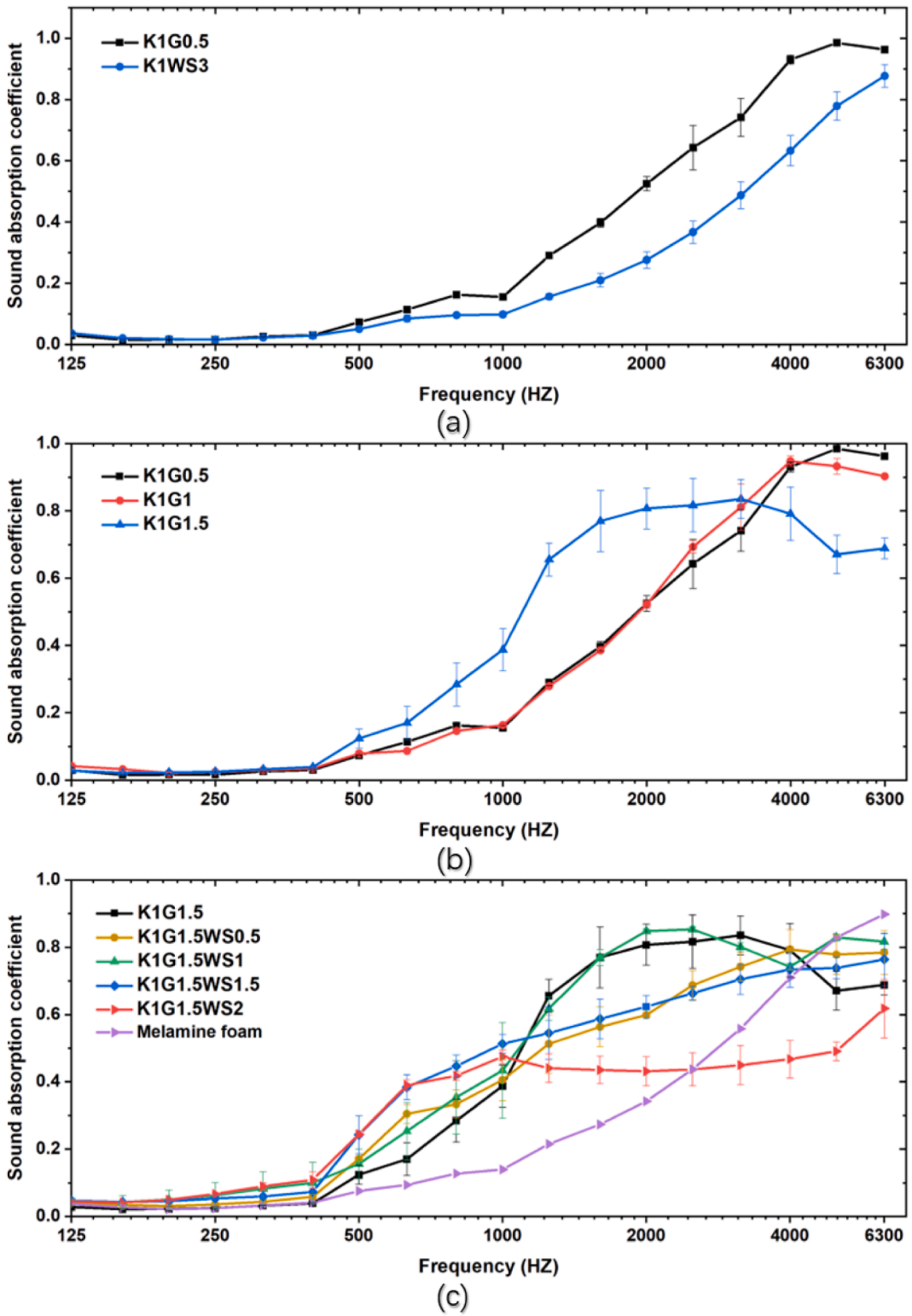

Fig. 7. Sound absorption efficient of composite aerogels with thickness of 10 mm (a: K1G0.5, K1WS3); (b: K1G0.5, K1G1, K1G1.5) and (c: K1G1.5, K1G1.5WS0.5, K1G1.5WS1, K1G1.5WS1.5, K1G1.5WS2 and melamine foam with thickness of 25 mm).

fine pores existing on the surface and inside of the KGM/gelatin aerogels. As illustrated in Fig. 8 (a), the pores are connected to one another and communicate with the outside, so the aerogel is air permeable and easy for sound waves to enter. When the sound waves travel through the aerogels, friction is generated between the waves and the internal complex pore structures of aerogels, resulting in viscosity and heat conduction effects, and the sound energy is gradually turned into heat dissipation after a long path. Therefore, KGM/gelatin aerogels have better sound absorption performance. As shown in Fig. 7 (b), it is observed to exhibit an improvement in sound absorption performance with the increase of gelatin concentrations. With frequencies ranging from 125 to 6300 Hz, the NRC values of K1G0.5, K1G1 and K1G1.5 are 0.29, 0.30 and 0.36, respectively. The improvement is caused by the increasing number and proportion of small size pores as shown in Figs. 3

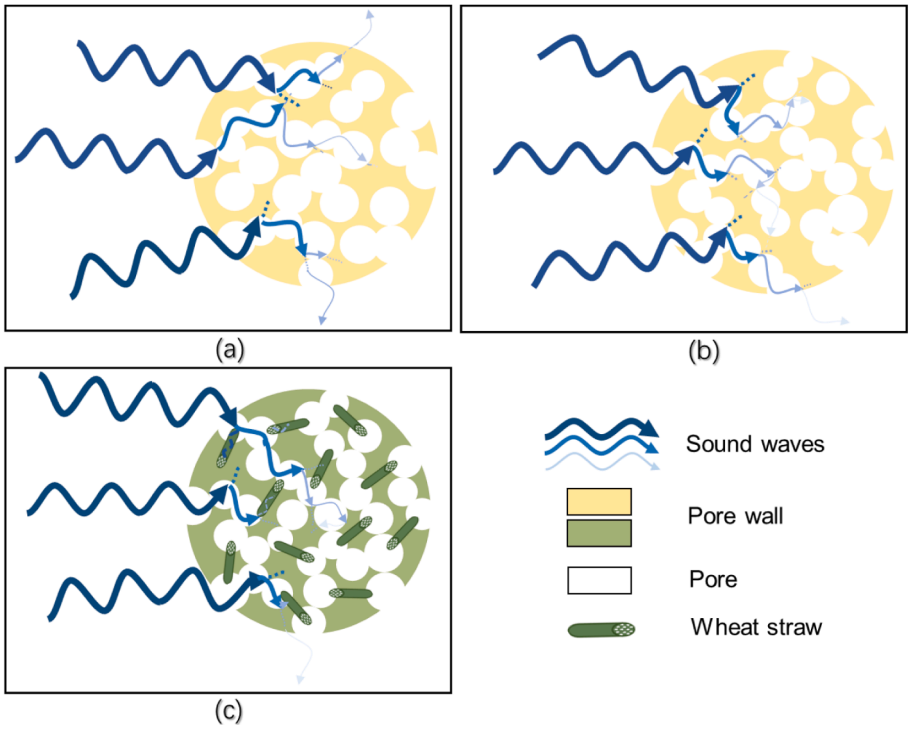

Fig. 8. Illustration of sound absorption by (a) K1G0.5, (b) K1G1.5 and (c) K1G1.5WS1.

and 4, which enhance the complexity of pore structure and cause more reflection and friction between the pore walls and sound waves. This increases the energy loss during the propagation of sound waves, as illustrated in Fig. 8 (b). It is noteworthy that although the NRC of K1G1.5 is the highest among three KGM/gelatin aerogels, there is a decrease in the absorption coefficient from 0.79 at 4000 Hz to 0.67 at 5000 Hz. It may be explained by that the flow resistance of K1G1.5 is increased due to more total solid content, and it has a negative effect on the high-frequency sound.

To further improve the sound absorption performance of KGM-based aerogels, it is necessary to reduce the internal flow resistance of K1G1.5 aerogels. As verified in previous study [37,43], the resistance of KGM-based aerogels shows a significant reduction with the addition of wheat straw as it has multi-cavity and hollow structure, which could help to dissipate the energy of sound waves, as illustrated in Fig. 8 (c). Meanwhile, gelatin can prevent the subsidence of wheat straw as it can be converted into gel rapidly below 37 °C. It is observed from Fig. 7 (c) that the introduced wheat straw has an influence on the sound absorption coefficient which can be clearly reflected by the NRC values. The NRC values of the KGM/gelatin/wheat straw aerogels with wheat straw addition from 0 to 2% are 0.36, 0.34, 0.38, 0.37 and 0.29, respectively. To have a comparison, widely used melamine foams with thickness of 25 mm but different diameters of 30 mm and 96 mm were tested to obtain sound absorption coefficient at different frequency ranges, and the sound absorption coefficient (NRC 0.22) is shown in Fig. 7 (c). Below 4000 Hz, the sound absorption coefficient of melamine foam with 25 mm thickness is much lower than that of KGM-based aerogels with 10 mm thickness, which shows excellent sound absorption characteristics. At low and medium frequencies, it can be found that sound absorption coefficient of KGM/gelatin/wheat straw aerogels is slightly raised when the wheat straw content increases from 0 to 2.00%. This is in accordance with the rule, that is, when the thickness of the material is maintained at

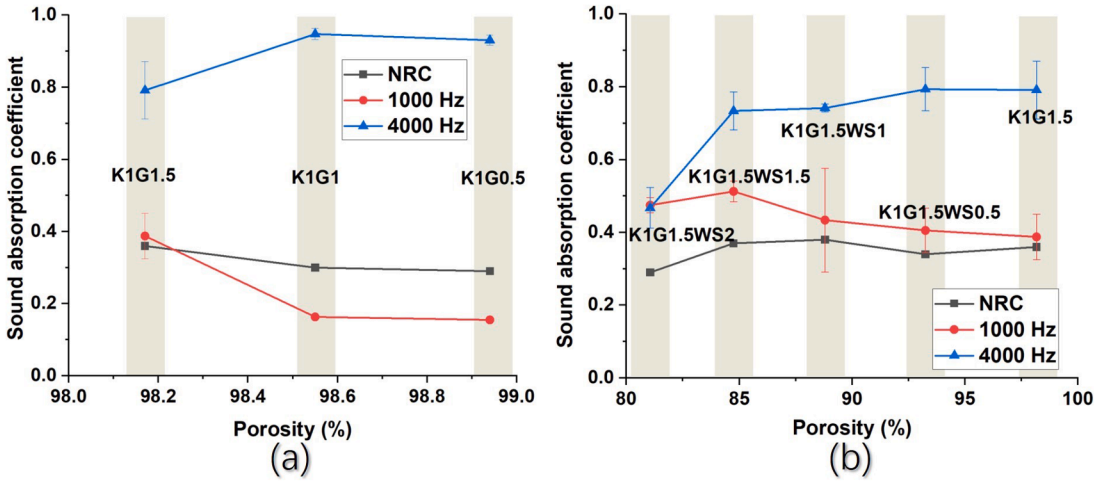

Fig. 9. Effect of porosity on the sound absorption coefficient of (a) KGM/gelatin aerogels and (b) KGM/gelatin/wheat straw aerogels.

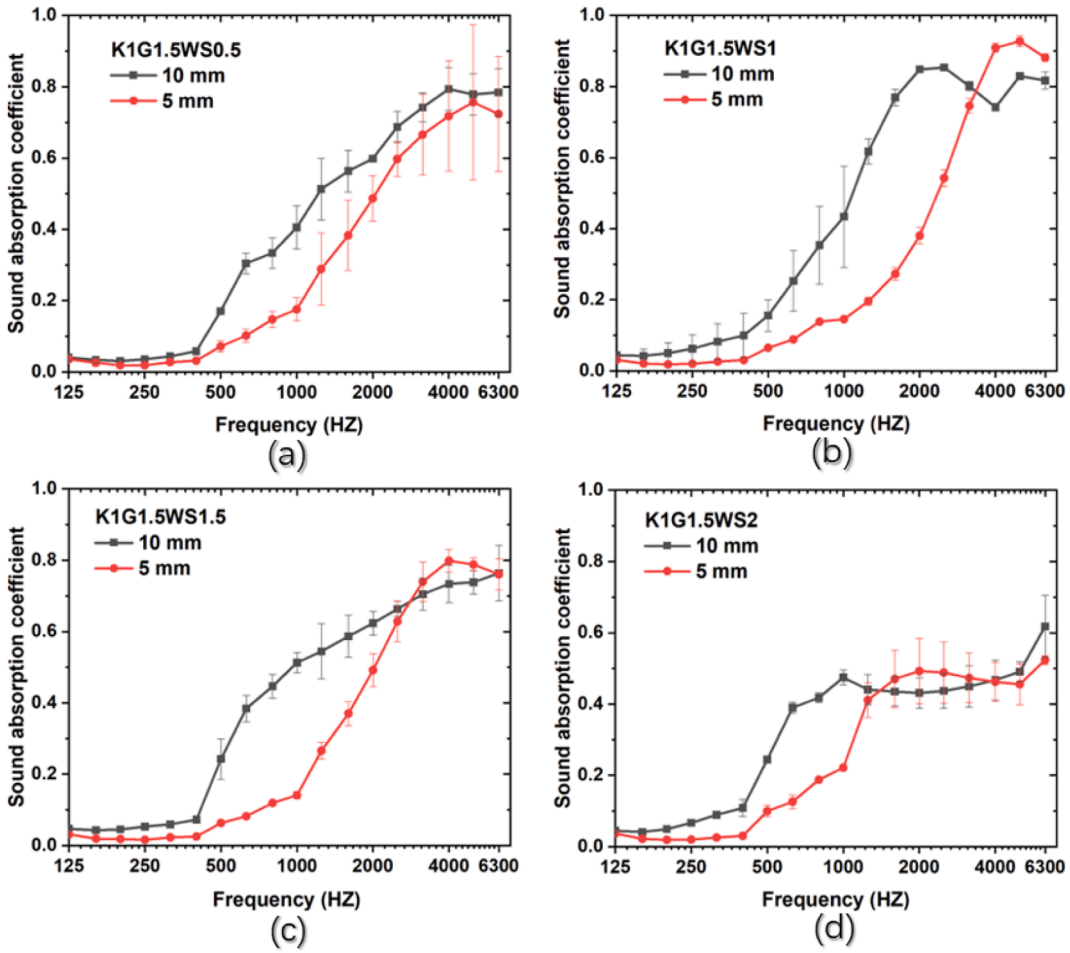

Fig. 10. Effect of thickness on the sound absorption coefficient of KGM/gelatin/wheat straw aerogels.

a certain level, increasing material density can slightly improve sound absorption coefficient at low and medium frequencies [44]. When the wheat straw addition increases from 0 to 0.50%, the sound absorption values at high frequencies present a slight decrease, which may be explained by that a very small amount of wheat straw addition is not sufficient to achieve the function to reduce the flow resistance inside KGM-based aerogel. As can be seen in Fig. 7 (c), the sound absorption coefficient of K1G1.5WS1 in the high frequency range is the highest among all KGM/gelatin/wheat straw aerogels. Since the wheat straw content continues to rise, especially when the wheat straw concentration reaches 2.00%, the sound absorption coefficient decreases significantly at high frequencies as a large amount of wheat straw causes high flow resistance. Therefore, appropriate small amount of wheat straw addition contributes to the improvement of sound absorption performance.

As there is a change in porosity with different additions of gelatin and wheat straw, the effect of porosity on NRC, sound absorption coefficients at 1000 Hz and 4000 Hz are investigated for KGM/gelatin aerogels and KGM/gelatin/wheat straw aerogels separately, as shown in

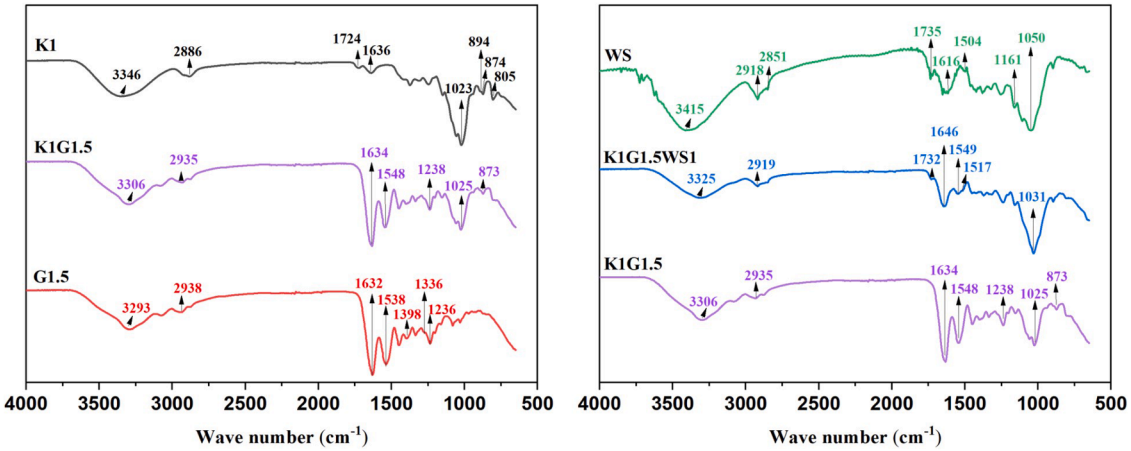

Fig. 11. FTIR spectra of KGM aerogel, gelatin aerogel, wheat straw and KGM-based aerogel.

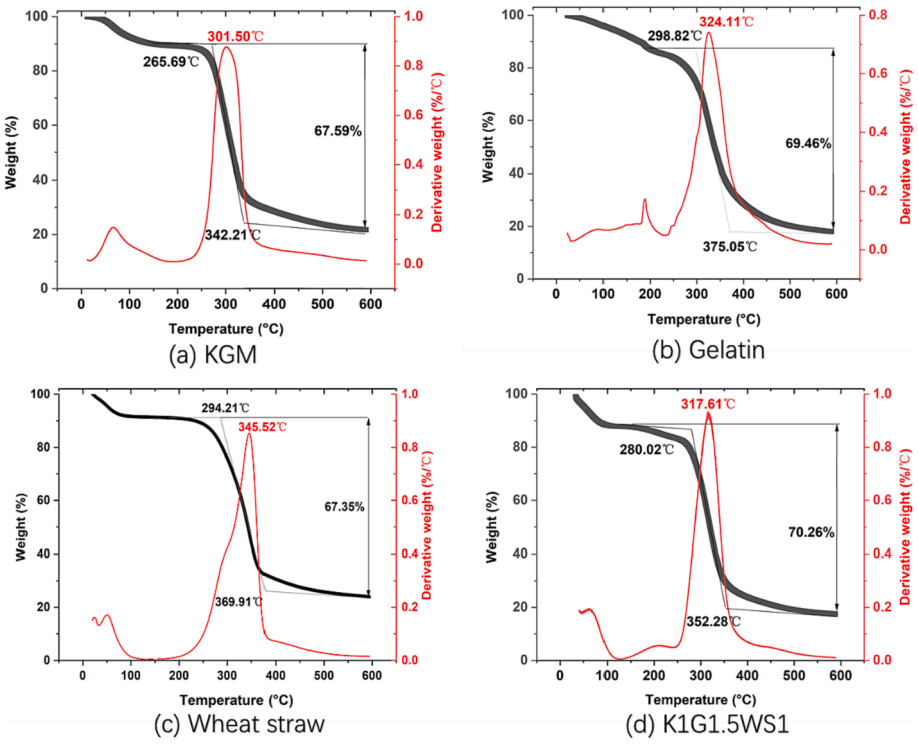

Fig. 12. TGA of KGM, gelatin, wheat straw and K1G1.5WS1 aerogel.

Fig. 9. Results present that with the increase in porosity of both KGM/gelatin aerogels and KGM/gelatin/wheat straw aerogels, the sound absorption coefficient at 1000 Hz has a decreasing trend, while the coefficient at 4000 Hz has an increasing trend. This indicates that the increased porosity has a positive influence on the sound absorption performance at high frequency. However, the effect of porosity on the NRC value is not obvious as NRC is an average value of sound absorption coefficients from low to high frequencies.

Fig. 10 shows the influence of thickness on the sound absorption coefficient of KGM-based aerogels with different wheat straw additions. As shown in Fig. 10, the sound absorption coefficient gradually increases with the increase of thickness, especially in the low frequency range. The increased thickness also leads to the shifting of peak sound absorption coefficient towards lower frequencies. The results have good agreement with the review by Dunne et al. [45].

According to the investigation of sound absorption performance, it could be summarized that the addition of gelatin could enhance the sound absorption property of KGM-based aerogels as it could generate more fine pores in aerogels. With further addition of wheat straw in aerogels, the sound absorption property can be improved due to the unique cavity structure of wheat straw. With the addition of gelatin and wheat straw, the porosity changes and has a positive influence on the sound absorption performance at high frequencies. Differently, the thickness plays a role in the improvement of sound absorption performance at low frequencies.

3.3. Infrared reflectance spectroscopy of KGM-based aerogels

FTIR is used to analyze the chemical groups of the KGM-based aerogels. As shown in Fig. 11, KGM FTIR spectral features can be observed at 874 cm^{-1} and 805 cm^{-1}, and the peak at around 894 cm^{-1} is associated with the β-glucosidic bonds in KGM. These characteristic absorption bands are also exhibited in KGM/gelatin aerogels, which indicates the characteristic structure of KGM is not impaired. KGM aerogel also shows peaks at 1636 cm^{-1} corresponding to the C—O stretching of the hydroxyl group [46]. For gelatin aerogel, the characteristic peak at 1632 cm^{-1} is attributed to the amide I extension of C═O and the peak situated at 1538 cm^{-1} can be assigned to the amide II stretching of C—N and bending of the N—H ligation. Spectral peak at 1236 cm^{-1} results from the amide III (the plane vibration of C—N and N—H bond) [47]. Compared with spectrum of gelatin aerogel, some peaks of KGM/gelatin aerogels become slightly stronger and the peaks for amide I, II, and III of KGM/gelatin aerogels shift to the higher wavenumbers due to the addition of KGM. Generally, intermolecular interactions of chemical groups are reflected in FTIR spectra, such as the absorption bands shifts, which may represent hydrogen bond interactions between KGM and gelatin chains. Two dominant absorption peaks of wheat straw are distributed at around 3415 cm^{-1} and 1050 cm^{-1}, which come from the stretching vibrations of OH and CO, respectively [48]. The peak at 1616 cm^{-1} is a characteristic absorption band of lignin, caused by the vibration of the aromatic backbone [25]. Typical chemical bonding behaviors of aromatic rings C═C stretch of lignin is observed in the area around 1504 cm^{-1}. In K1G1.5WS1, a broad peak at 3325 cm^{-1} and a narrow peak at 1031 cm^{-1} are presented and shift to a higher wave number compared with KGM/gelatin aerogels, which may be caused by the formation of hydrogen bond. These results indicate the good miscibility between polymers.

3.4. Thermal property of KGM-based aerogels

Fig. 12 shows the TGA results of KGM-based aerogels. The thermal decomposition of all aerogels has mainly-two stages. The first degradation stage is from a temperature of 20 °C to about 100 °C, corresponding to the evaporation of free and bound water in the sample. The mass loss in the second stage starts from around 100 °C, which mainly originates from the breakage of glycosidic bonds in the polysaccharides and the degradation of amino acids in the proteins. For KGM aerogels, the main decomposition temperatures range from 265.69 °C to 342.21 °C, which is lower than the ones of gelatin (298.82–375.05 °C) and wheat straw (294.21–369.91 °C). For wheat straw, the temperature where the maximum thermal decomposition rate appears is the highest (345.52 °C) among all components, which may be attributed to its

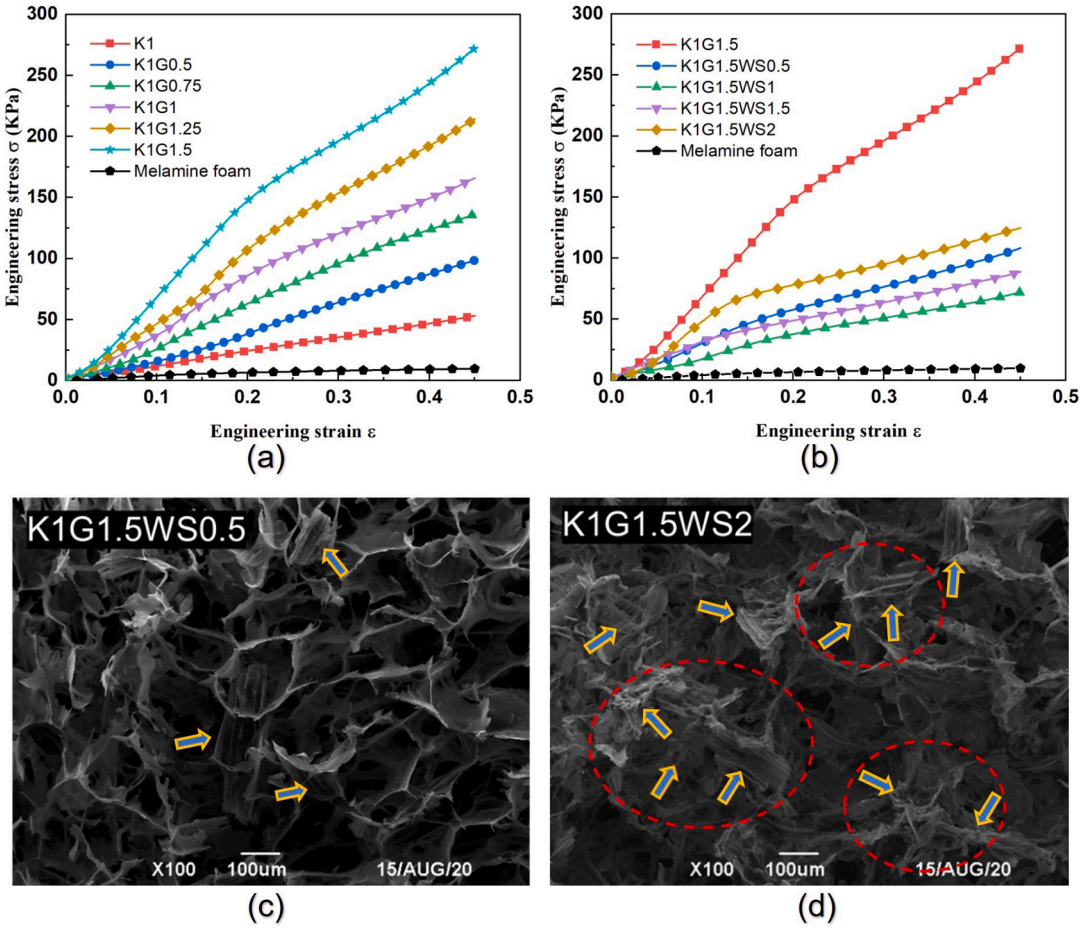

Fig. 13. Compressive testing results of KGM-based aerogels with different additions of (a) gelatin and (b) wheat straw and the comparison with melamine foam [49]; SEM observation of wheat straw distribution in (c) K1G1.5WS0.5 and (d) K1G1.5WS2.

special cavity structure that hinders heat transfer to some extent. After the addition of wheat straw, the mass loss of K1G1.5WS1 ranges from 280.02 to 352.28 °C, where about 70.26% of the weight was lost due to the degradation of polysaccharides, gelatin, and wheat straw. As shown in Fig. 12, the epitaxial initial decomposition temperature of K1G1.5WS1 is observed to be between the temperatures of three pure components. The results indicate that the thermal stability of KGM-based aerogels with addition of gelatin and wheat straw could maintain a relatively good level compared to raw materials.

3.5. Mechanical behavior

In order to be used in buildings for sound absorption, the novel sound absorption material should have acceptable loading capacity to external mechanical forces. The mechanical property of the developed KGM-based aerogel with addition of gelatin and wheat straw is of great value to be investigated. In this study, the compressive behaviors of KGM-based aerogels with different additions of gelatin and wheat straw were tested. As the stress – strain curves were obtained from continuous tests, only one representative curve for each aerogel material is presented, which is the intermediate one among results of three repeated tests. As shown in Fig. 13 (a and b), the compressive behavior presents a nonlinear stress–strain relationship with different stages: linear elastic, plateau, and densification stages, although the latter two stages are not significantly obvious. It can also be observed that the additions of gelatin and wheat straw have different effect on the strength of KGM-based aerogels. Between them, the gelatin plays a positive role in strengthening the KGM-based aerogel because gelatin itself is stronger than KGM. With the increase of gelatin addition, the pore size of KGM-based aerogels becomes smaller, and the wall thickness becomes slightly larger, which is revealed by Figs. 3 and 5 in Section 3.1. Meanwhile, the strength of KGM-based aerogel presents to decrease first and then increase with the addition of wheat straw. As marked by arrows in Fig. 13 (c), a small number of wheat straws are hugged by pore walls and this unique combination may have negative effect on the structural stability, which causes the worse mechanical property. With more wheat straw addition, the interaction effect among wheat straws becomes more obvious and tiny wheat straw bars support one another to form nest structures as marked by red dashed lines, which are more stable than the original structures. Although the inherent negative influence of wheat straw still exists, the nest structure can lead to the strengthening effect when a large number of wheat straws are added. This explains the unique mechanical behavior variation when different wheat straw additions are used. Compared with widely used melamine foam [49], all the developed KGM-based aerogels show much higher strength, which indicates that the mechanical properties qualify the developed aerogels to be used in building applications.

The investigation of compressive behavior of KGM-based aerogels reveals that gelatin plays a positive role in strengthening KGM-based aerogels due to the refined pore structure and thicken pore walls. However, the effect of wheat straw is more complicated. With a small amount of wheat straw addition, unstable structure firstly appears and weakens the aerogels because of the random distribution of wheat straw bars, while a more stable nest structure could be formed to strengthen the aerogels with more wheat straw added.

3.6. Mechanical modelling of the compressive behavior

To predict the compressive behavior for potential loading capacity evaluation and to benefit the material design, a model is proposed for KGM-based aerogels with different additions of gelatin and wheat straw. This model is comprised of three parts to describe stress – strain relationship, the effects of gelatin addition and wheat straw addition. During the modelling process, the coefficient of determination (R^2) and root mean square error (*RMSE*) are used to evaluate the prediction accuracy, the calculation equations of which are given as below:

$$R^2 = \left[\sum_{i=1}^{N}(E_i - E_m)^2 - \sum_{i=1}^{N}(E_i - P_i)^2\right] \Big/ \sum_{i=1}^{N}(E_i - E_m)^2 \tag{2}$$

$$RMSE = \sqrt{1/N\sum_{i=1}^{N}(E_i - P_i)^2} \tag{3}$$

where, E_i is the experimental values; E_m is the mean value, which is the average of all the experimental data; P_i is the predicted value; and N is total number of experimental cases used in the evaluation process. A higher level of R^2 value and/or a lower level of *RMSE* value indicate better prediction accuracy of the mechanical model.

3.6.1. Function to describe stress – Strain relationship

Three different models are tested and compared in the current study: polynomial model [50], Ogden model [51] and Yeoh model [52]. The polynomial model is initially proposed to describe the elasticity of rubber-like incompressible materials and is dependent of two strain invariants I_1, I_2 of the left Cauchy-Green deformation tensor [50]. While, for compressible materials, such as KGM-based aerogel in this study, the strain energy density W can be expressed as following:

$$W = \sum_{i,j=0}^{n} C_{ij}(\bar{I}_1 - 3)^i(\bar{I}_2 - 3)^j + \sum_{i=1}^{n} D_i(J-1)^{2i} \tag{4}$$

where, $\bar{I}_1 = J^{-2/3}I_1$, $\bar{I}_2 = J^{-4/3}I_2$, $I_1 = \lambda_1^2 + \lambda_2^2 + \lambda_3^2$, $I_2 = \lambda_1^2\lambda_2^2 + \lambda_2^2\lambda_3^2 + \lambda_3^2\lambda_1^2$, $J = \det(F)$, F is the deformation gradient, C_{ij}, D_i are model parameters and $C_{00} = 0$, and n is the parameter to determine the term number and order in the model. λ_1, λ_2 and λ_3 are stretch ratios, which are defined as the ratio between the lengths after and before deformation. For both uniaxial tensile and compressive tests, they can be expressed by the parallel stretch ratio λ as: $\lambda_1 = \lambda$ and $\lambda_2 = \lambda_3 = \lambda^{-1/2}$ [53]. As the strain energy density is defined as the strain energy per unit volume, the relationship between the engineering stress σ and the strain energy density W for uniaxial deformation state can be formulated as Eq. (5):

$$\sigma = \frac{\partial W}{\partial \lambda} \tag{5}$$

According to Eqs. (4) and (5), the relationship between the engineering stress σ and the stretch ratio λ is derived and can be finally expressed as following equation:

$$\sigma = 2\left(\lambda - \lambda^{-2}\right)\left[C_{10} + C_{01}\lambda^{-1} + 2C_{20}\left(\lambda^2 + 2\lambda^{-1} - 3\right) + 2C_{20}\left(2\lambda + \lambda^{-2} - 3\right) + 3C_{11}\left(\lambda - 1 - \lambda^{-1} + \lambda^{-2}\right)\right] \tag{6}$$

where, the conversion from stretch ratio λ to engineering strain ε can be easily achieved by using the relationship of $\lambda = 1 + \varepsilon$ for tensile testing condition and $\lambda = 1 - \varepsilon$ for compressive testing condition.

Ogden model also has a strain energy density function to describe the non-linear behavior of materials such as rubbers, polymers and biological tissue [51]. For compressible materials, the strain energy density W is expressed as the following format:

$$W = \sum_{i=1}^{n} \frac{\mu_i}{\alpha_i}\left(\lambda_1^{\alpha_i} + \lambda_2^{\alpha_i} + \lambda_3^{\alpha_i} - 3\right) + \sum_{i=1}^{n} D_i(J-1)^{2i} \tag{7}$$

The engineering stress – stretch ratio relationship under Ogden model can be derived and written as the following equation:

$$\sigma = \lambda^{-2}\left(\mu_1\lambda^{\alpha_1} + \mu_2\lambda^{\alpha_2} - \mu_1\lambda^{-1/2\alpha_1} - \mu_2\lambda^{-1/2\alpha_2}\right) \tag{8}$$

Yeoh model is a reduced polynomial model. The same to the above two models, Yeoh model also has the assumption that the material behavior can be described by using a function of the strain energy density W [52], which can be expressed as following for compressible materials:

$$W = \sum_{i=1}^{n} C_{i0}(\bar{I}_1 - 3)^i + \sum_{i=1}^{n} D_i(J-1)^{2i} \tag{9}$$

where, $n = 3$, and C_{i0} is model parameter.

Therefore, the engineering stress can be predicted by Yeoh model using the following equation:

$$\sigma = 2C_{10}\left(\lambda - \lambda^{-2}\right) + 4C_{20}\left(\lambda - \lambda^{-2}\right)\left(\lambda^2 + 2\lambda^{-1} - 3\right) + 6C_{30}\left(\lambda - \lambda^{-2}\right)\left(\lambda^2 + 2\lambda^{-1} - 3\right)^2 \tag{10}$$

To test and compare the applicability of the above three models, the compressive testing result of K1G1.5 is used in this study. The parameters of the polynomial, Ogden and Yeoh models are calculated and given in Table 1.

Table 1
Parameters of the polynomial, Ogden and Yeoh models.

Model	Parameter	Value
Polynomial model	C_{10}(KPa)	−434.63
	C_{01}(KPa)	504.84
	C_{20}(KPa)	−1337.51
	C_{11}(KPa)	1202.39
	C_{02}(KPa)	−325.71
Ogden model	μ_1(KPa)	1112.05
	α_1	−0.8962
	μ_2(KPa)	−926.46
	α_2	−1.45
Yeoh model	C_{10}(KPa)	95.39
	C_{20}(KPa)	−31.37
	C_{30}(KPa)	3.63

Fig. 14 (a and b) shows the prediction results and the comparison between different models tested in this study. From Fig. 14 (a), it is clearly shown that the polynomial model can give better prediction result than the other two models. From the quantitative aspect, the prediction result of the polynomial model has the highest R^2 and lowest *RMSE* level of 0.9997 and 1.515 MPa, respectively, while Ogden and Yeoh models present relatively worse prediction effect. Therefore, in the proposed model, the polynomial model is considered to act as the part to describe the stress – strain relationship.

3.6.2. Effect of gelatin addition

As shown in Fig. 14 (c), the engineering stress for different addition of gelatin at the same engineering strain of 0.45 is extracted from Fig. 13 (a), and the experimental results clearly indicate that the addition of gelatin has an enhancement effect on the strength of KGM-based aerogels. Moreover, with the increase of gelatin concentration, the enhancement effect is observed to be more obvious. Based on the above experimental observation, the following phenomenological equation is proposed to predict the effect of gelatin addition on the engineering stress σ of KGM-based aerogel:

$$\sigma = \sigma_G^{Ref}\exp\left[k\left(\rho_G - \rho_G^{Ref}\right)\right] \tag{11}$$

where, ρ_G is the addition of gelatin, ρ_G^{Ref} is the selected reference addition of gelatin, σ_G^{Ref} is the engineering stress of KGM-based aerogel with reference gelatin addition and k is the model parameter. The gelatin addition of 1.50% is selected as the reference value before the parameter identification, and therefore σ_G^{Ref} is observed to be 307.39 KPa. By fitting the experimental relationship between the engineering

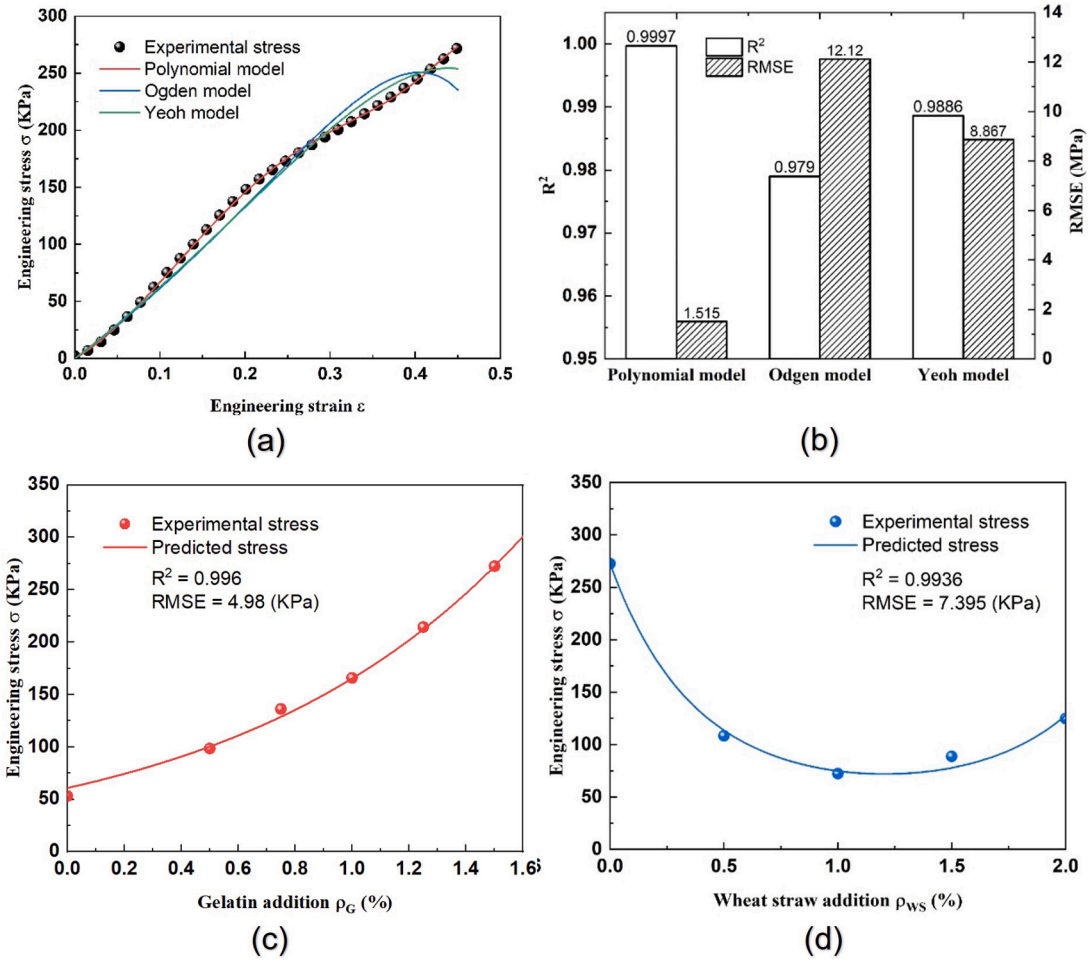

Fig. 14. Comparison between different models: (a) predicted stress – strain curves and (b) calculated R^2 and *RMSE*; Experimental and predicted effects of (c) gelatin addition and (d) wheat straw addition on engineering stress.

stress and the gelatin addition, the model parameter k is identified as 99.87 in the studied case.

As shown in Fig. 14 (c), with the use of Eq. (11), the predicted results are presented by the red curve. It is observed that the predicted results are in good agreement with the experimental results, and R^2 and *RMSE* have values of 0.996 and 4.98 KPa, respectively, which indicate that an accurate prediction of the effect of gelatin addition is achieved.

3.6.3. *Effect of wheat straw addition*

In experiment, the effect of wheat straw addition on the engineering stress of KGM-based aerogels is presented in Fig. 14 (d). The engineering stress for different additions of wheat straw is extracted from Fig. 13 (b) at the same strain of 0.45. Initially, the addition of wheat straw significantly reduces the strength of KGM-based aerogels. With the wheat straw addition of 1.00%, the worst strength is observed. However, the strength tends to be enhanced when the addition of wheat straw continues to increase after 1.00% addition of wheat straw and with addition of 1.50%, an obvious increasement of strength is reached. To predict the unique trend of the effect of wheat straw addition, the following equation is proposed:

$$\sigma = \sigma_{WS}^{Ref}\exp\left[m\left(\rho_{WS}-\rho_{WS}^{Ref}\right)+n\left(\rho_{WS}-\rho_{WS}^{Ref}\right)^2\right] \quad (12)$$

where, ρ_{WS} is the addition of wheat straw, ρ_{WS}^{Ref} is the selected reference addition of wheat straw, σ_{WS}^{Ref} is the engineering stress of KGM-based aerogel with the reference wheat straw addition, m and n are model parameters. The wheat straw addition of 0% is selected as the reference value, and therefore σ_{WS}^{Ref} is observed to be 307.39 KPa, which is the same to σ_{G}^{Ref}. The experimental relationship between the engineering stress and the wheat straw addition gives the fitting results of model parameters m and n, which are identified as −220.7 and 9144, respectively.

With the above proposed Eq. (12) and identified values of model parameters, the predicted results of the effect of wheat straw addition are depicted as the blue curve in Fig. 14 (d). Results show that the proposed equation can predict the effect of wheat straw addition and reflect the unique weakening trend followed by a hardening effect. The values of R^2 and *RMSE* are calculated as 0.9936 and 7.395 KPa, respectively, which demonstrate the high accuracy of the proposed prediction equation.

Table 2
Parameters of the prediction model for compressive behavior of KGM-based aerogels with different additions of gelatin and wheat straw.

Parameter	Value
C_{10}(KPa)	−434.63
C_{01}(KPa)	504.84
C_{20}(KPa)	−1337.51
C_{11}(KPa)	1202.39
C_{02}(KPa)	−325.71
k	99.87
m	−220.70
n	9144

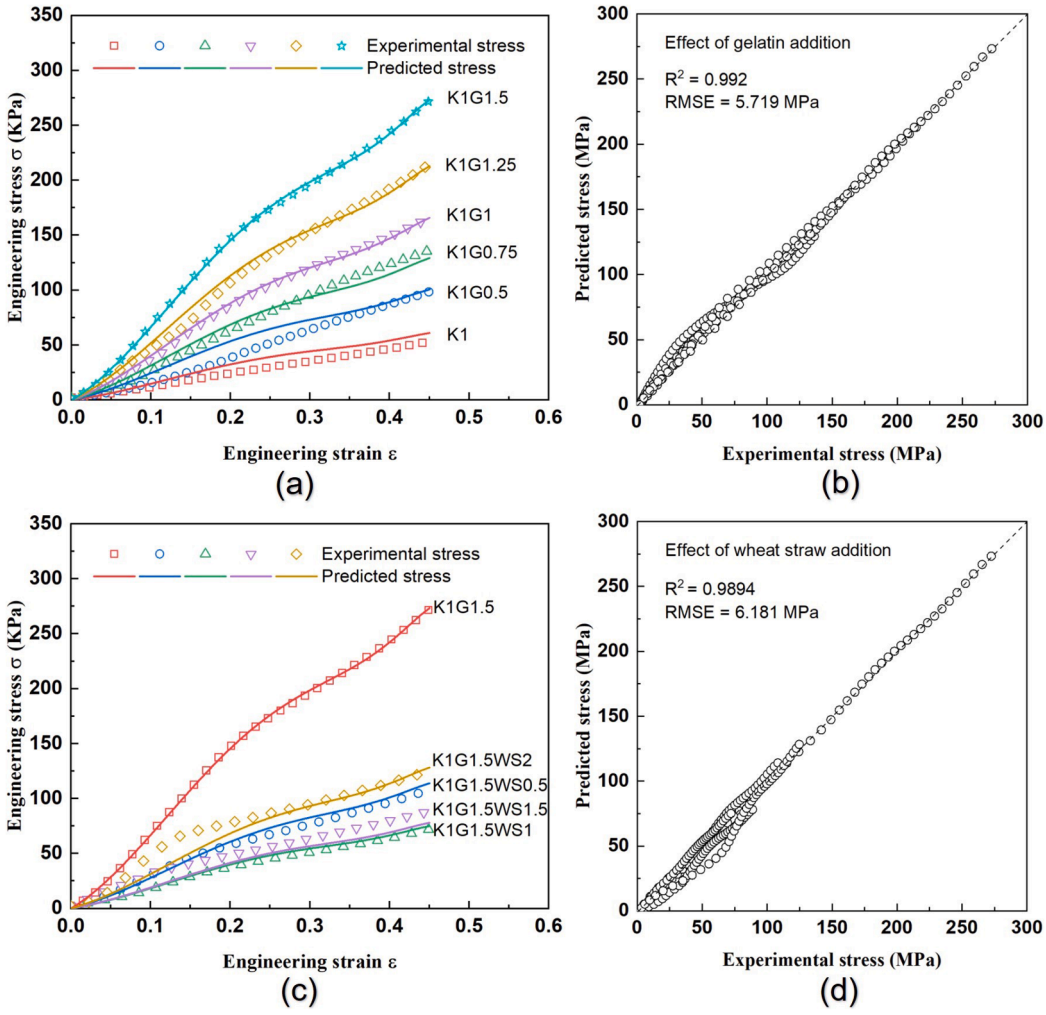

Fig. 15. Prediction and evaluation results of the mechanical model for compressive behavior of KGM-based aerogels with different additions of (a), (b) gelatin, (c) and (d) wheat straw.

3.6.4. Mechanical model and prediction results

To summarize, the prediction model for the compressive behavior of the studied KGM-based aerogels can be written as the following equation:

$$\sigma = 2\left(\lambda-\lambda^{-2}\right)\left[C_{10}+C_{01}\lambda^{-1}+2C_{20}\left(\lambda^{2}+2\lambda^{-1}-3\right)+2C_{20}\left(2\lambda+\lambda^{-2}-3\right)+3C_{11}\left(\lambda-1-\lambda^{-1}+\lambda^{-2}\right)\right]\exp\left[k\left(\rho_{G}-\rho_{G}^{Ref}\right)+m\left(\rho_{WS}-\rho_{WS}^{Ref}\right)+n\left(\rho_{WS}-\rho_{WS}^{Ref}\right)^{2}\right] \quad (13)$$

where, the model parameters are summarized in Table 2. In this model, the reference values of gelatin and wheat straw additions are 1.5% and 0%, respectively.

Using the derived model parameters, the prediction results are presented in Fig. 15 (a and c) for different additions of gelatin and wheat straw. For the prediction results of different gelatin additions shown in Fig. 15 (a), although it shows a slight degree of difference from the experimental curve of K1G0.5 at small strain range, all other predicted curves have high agreement with the experimental ones. Meanwhile, for the prediction results of different wheat straw additions shown in Fig. 15 (c), the ones of wheat straw addition of 1.50% and 2.00% are observed to be less accurate compared to other three cases, but the unique effect of wheat straw addition on the compressive behavior is presented successfully. The R^2 values of these two parts of prediction are calculated as 0.992 and 0.9894, respectively, which mean the model is capable of predicting the compressive behavior of KGM-based aerogels with different additions of gelatin and wheat straw with high accuracy.

4. Conclusions

This study demonstrates new KGM-based aerogels with promising sound absorption property, which are expected to be mainly used as interior wall/ ceiling panels for sound absorption in such as studios, halls, theatres and stadiums, and core materials of sandwich composite walls/ lightweight panels to enhance sound insulation in such as conference rooms, hotels, factories and temporary buildings. The raw materials used to produce this material are natural, renewable, and more importantly, the waste wheat straw is converted to a valuable raw material. The pore structure, sound absorption property, infrared reflectance spectroscopy, thermal and mechanical properties of KGM-based aerogels are investigated and presented, followed by a mechanical model to predict the compressive behavior. The main conclusions are drawn as follows:

(1) The additions of gelatin contribute to the increase in number and proportion of small open pores, which is the main reason for the improvement of sound absorption property of KGM-based aerogels. Wheat straw has unique multi-cavity structure and appropriate little addition can improve the sound absorption performance of KGM-based aerogels because this structure can work along with the pore structure to absorb energy of sound waves.

(2) The NRC values of KGM-based aerogels are tested to be between 0.29 and 0.38. The optimized KGM-based aerogel specimen for sound absorption is identified to be K1G1.5WS1, with the NRC value of 0.38. Compared with melamine foam, better sound absorption performance can be achieved by the developed KGM-based aerogels.
(3) The thermal decomposition property of KGM-based aerogels is similar to the ones of three raw materials. The initial decomposition temperature of the K1G1.5WS1 aerogel is identified to be moderate among the temperatures of KGM, gelatin and wheat straw. A relatively good level of thermal stability is maintained in the composite aerogels.
(4) The developed KGM-based aerogels have qualified mechanical property to be used as interior wall, ceiling panels, core materials of sandwich walls and lightweight panels in buildings. A nonlinear compressive behavior is observed with different stages. Gelatin has a positive influence on strengthening KGM-based aerogel, and smaller pore size and larger wall thickness are induced by the increased addition of gelatin. With the addition of wheat straw, the strength of KGM-based aerogel is first weakened obviously and then increases when the addition is more than 1.00%. This results from the unstable structure due to the distribution of wheat straw hugged by pore walls, while with the increased addition the high-intensity fine wheat straws interact each other and form a more stable nest structure to strengthen KGM-based aerogels.
(5) The proposed mechanical model is capable of predicting the compressive stress–strain curves of KGM-based aerogels with high accuracy. The additions of gelatin and wheat straw are considered in this model, and it is proven to be effective in predicting the effect of gelatin and wheat straw on the compressive behavior.

CRediT authorship contribution statement

Yixin Wang: Conceptualization, Data curation, Formal analysis, Investigation, Methodology, Visualization, Writing – original draft. **Hui Zhu:** Conceptualization, Formal analysis, Investigation, Methodology, Validation, Visualization, Writing – review & editing. **Wenyao Tu:** Data curation, Validation. **Yuehong Su:** Resources, Supervision. **Fatang Jiang:** Conceptualization, Funding acquisition, Resources. **Saffa Riffat:** Supervision.

Declaration of Competing Interest

The authors declare that they have no known competing financial interests or personal relationships that could have appeared to influence the work reported in this paper.

Data availability

The data that has been used is confidential.

Acknowledgements

This work was financially supported by National Natural Science Foundation of China (Grant No.: 31972156) and the European Commission for the H2020 Marie Skłodowska-Curie Actions Individual Fellowships-2017 Project (Grant No.: 794680).

References

[1] B. Basu, E. Murphy, A. Molter, A. Sarkar Basu, S. Sannigrahi, M. Belmonte, F. Pilla, Investigating changes in noise pollution due to the COVID-19 lockdown: The case of Dublin, Ireland, Sustain. Cities Soc. 65 (2021), 102597.
[2] G. Ma, M. Yang, S. Xiao, Z. Yang, P. Sheng, Acoustic metasurface with hybrid resonances, Nat. Mater. 13 (9) (2014) 873–878.
[3] F. Setaki, M. Tenpierik, M. Turrin, A. van Timmeren, Acoustic absorbers by additive manufacturing, Build. Environ. 72 (2014) 188–200.
[4] Y. Zhang, H. Li, A. Abdelhady, H. Du, Laboratorial investigation on sound absorption property of porous concrete with different mixtures, Constr. Build. Mater. 259 (2020), 120414.
[5] B. Ma, Z. Jin, Y. Su, W. Lu, H. Qi, P. Hu, Utilization of hemihydrate phosphogypsum for the preparation of porous sound absorbing material, Constr. Build. Mater. 234 (2020), 117346.
[6] H. Gao, H. Liu, L. Liao, L. Mei, F. Zhang, L. Zhang, S. Li, G. Lv, A bifunctional hierarchical porous kaolinite geopolymer with good performance in thermal and sound insulation, Constr. Build. Mater. 251 (2020), 118888.
[7] M.Z.H. Mahmud, N.A. Hassan, M.R. Hainin, C.R. Ismail, R.P. Jaya, M.N.M. Warid, H. Yaacob, N. Mashros, Characterisation of microstructural and sound absorption properties of porous asphalt subjected to progressive clogging, Constr. Build. Mater. 283 (2021), 122654.
[8] J. Yoon, H. Kim, T. Koh, S. Pyo, Microstructural characteristics of sound absorbable porous cement-based materials by incorporating natural fibers and aluminum powder, Constr. Build. Mater. 243 (2020), 118167.
[9] J. Wang, B. Du, Experimental studies of thermal and acoustic properties of recycled aggregate crumb rubber concrete, Journal of Building Engineering 32 (2020), 101836.
[10] H. Wu, T. Zhang, R. Pan, Y. Chun, H. Zhou, W. Zhu, H. Peng, Q. Zhang, Sintering-free preparation of porous ceramsite using low-temperature decomposing pore former and its sound-absorbing performance, Constr. Build. Mater. 171 (2018) 367–376.
[11] S.S. Kistler, Coherent Expanded Aerogels and Jellies, Nature 127 (1931) 741.
[12] L. Druel, R. Bardl, W. Vorwerg, T. Budtova, Starch Aerogels: A Member of the Family of Thermal Superinsulating Materials, Biomacromolecules 18 (12) (2017) 4232–4239.
[13] S. Zhang, J. He, S. Xiong, Q. Xiao, Y. Xiao, F. Ding, H. Ji, Z. Yang, Z. Li, Construction and Nanostructure of Chitosan/Nanocellulose Hybrid Aerogels, Biomacromolecules 22 (8) (2021) 3216–3222.
[14] S. Zhang, J. Feng, J. Feng, Y. Jiang, Formation of enhanced gelatum using ethanol/water binary medium for fabricating chitosan aerogels with high specific surface area, Chem. Eng. J. 309 (2017) 700–707.
[15] J. Zhu, F. Zhao, R. Xiong, T. Peng, Y. Ma, J. Hu, L. Xie, C. Jiang, Thermal insulation and flame retardancy of attapulgite reinforced gelatin-based composite aerogel with enhanced strength properties, Compos. A Appl. Sci. Manuf. 138 (2020), 106040.
[16] W. Yang, A.C.Y. Yuen, P. Ping, R.-C. Wei, L. Hua, Z. Zhu, A. Li, S.-E. Zhu, L.-L. Wang, J. Liang, T.B.Y. Chen, B. Yu, J.-Y. Si, H.-D. Lu, Q.N. Chan, G.H. Yeoh, Pectin-assisted dispersion of exfoliated boron nitride nanosheets for assembled bio-composite aerogels, Compos. A Appl. Sci. Manuf. 119 (2019) 196–205.
[17] P.T.T. Nguyen, N.H.N. Do, X.Y. Goh, C.J. Goh, R.H. Ong, P.K. Le, N. Phan-Thien, H. M. Duong, Recent Progresses in Eco-Friendly Fabrication and Applications of Sustainable Aerogels from Various Waste Materials, Waste Biomass Valorization 13 (4) (2022) 1825–1847.
[18] Y.X. Chen, S. Sepahvand, F. Gauvin, K. Schollbach, H.J.H. Brouwers, Q. Yu, One-pot synthesis of monolithic silica-cellulose aerogel applying a sustainable sodium silicate precursor, Constr. Build. Mater. 293 (2021), 123289.
[19] C.-W. Lou, X. Zhou, X. Liao, H. Peng, H. Ren, T.-T. Li, J.-H. Lin, Sustainable cellulose-based aerogels fabricated by directional freeze-drying as excellent sound-absorption materials, J. Mater. Sci. 56 (33) (2021) 18762–18774.
[20] K. Yin, P. Divakar, U.G.K. Wegst, Plant-Derived Nanocellulose as Structural and Mechanical Reinforcement of Freeze-Cast Chitosan Scaffolds for Biomedical Applications, Biomacromolecules 20 (10) (2019) 3733–3745.
[21] W. Wang, Y. Fang, X. Ni, K. Wu, Y. Wang, F. Jiang, S.B. Riffat, Fabrication and characterization of a novel konjac glucomannan-based air filtration aerogels strengthened by wheat straw and okara, Carbohydr. Polym. 224 (2019), 115129.
[22] R. Valentin, R. Horga, B. Bonelli, E. Garrone, F. Di Renzo, F. Quignard, FTIR Spectroscopy of NH3 on Acidic and Ionotropic Alginate Aerogels, Biomacromolecules 7 (3) (2006) 877–882.
[23] L. Chen, Y. Li, Q. Du, Z. Wang, Y. Xia, E. Yedinak, J. Lou, L. Ci, High performance agar/graphene oxide composite aerogel for methylene blue removal, Carbohydr. Polym. 155 (2017) 345–353.
[24] Y. Lu, Q. Sun, D. Yang, X. She, X. Yao, G. Zhu, Y. Liu, H. Zhao, J. Li, Fabrication of mesoporous lignocellulose aerogels from wood via cyclic liquid nitrogen freezing–thawing in ionic liquid solution, J. Mater. Chem. 22 (27) (2012) 13548–13557.
[25] H. Pu, X. Ding, H. Chen, R. Dai, Z. Shan, Functional aerogels with sound absorption and thermal insulation derived from semi-liquefied waste bamboo and gelatin, Environ. Technol. Innovation 24 (2021), 101874.
[26] N.H.N. Do, T.P. Luu, Q.B. Thai, D.K. Le, N.D.Q. Chau, S.T. Nguyen, P.K. Le, N. Phan-Thien, H.M. Duong, Heat and sound insulation applications of pineapple aerogels from pineapple waste, Mater. Chem. Phys. 242 (2020), 122267.
[27] D. Qiao, J. Lu, W. Shi, H. Li, L. Zhang, F. Jiang, B. Zhang, Deacetylation enhances the properties of konjac glucomannan/agar composites, Carbohydr. Polym. 276 (2022), 118776.
[28] T. Gurunathan, S. Mohanty, S.K. Nayak, A review of the recent developments in biocomposites based on natural fibres and their application perspectives, Compos. A Appl. Sci. Manuf. 77 (2015) 1–25.
[29] Y. Wang, K. Wu, M. Xiao, S.B. Riffat, Y. Su, F. Jiang, Thermal conductivity, structure and mechanical properties of konjac glucomannan/starch based aerogel strengthened by wheat straw, Carbohydr. Polym. 197 (2018) 284–291.
[30] K. Wu, Y. Fang, H. Wu, Y. Wan, H. Qian, F. Jiang, S. Chen, Improving konjac glucomannan-based aerogels filtration properties by combining aerogel pieces in

series with different pore size distributions, Int. J. Biol. Macromol. 166 (2021) 1499–1507.
[31] K. Wu, H. Wu, R. Wang, X. Yan, W. Sun, Y. Liu, Y. Kuang, F. Jiang, S. Chen, The use of cellulose fiber from office waste paper to improve the thermal insulation-related property of konjac glucomannan/starch aerogel, Ind. Crops Prod. 177 (2022), 114424.
[32] Y. Wang, F. Xiang, W. Wang, W. Wang, Y. Su, F. Jiang, S. Chen, S. Riffat, Sound absorption characteristics of KGM-based aerogel, International Journal of Low-Carbon Technologies 15 (3) (2020) 450–457.
[33] K.M. Hess, W.V. Srubar, Activating relaxation-controlled diffusion mechanisms for tailored moisture resistance of gelatin-based bioadhesives for engineered wood products, Compos. A Appl. Sci. Manuf. 84 (2016) 435–441.
[34] T. Peng, J. Zhu, T. Huang, C. Jiang, F. Zhao, S. Ge, L. Xie, Facile preparation for gelatin/hydroxyethyl cellulose-SiO2 composite aerogel with good mechanical strength, heat insulation, and water resistance, J. Appl. Polym. Sci. 138 (23) (2021) 50539.
[35] S. Van Vlierberghe, V. Cnudde, P. Dubruel, B. Masschaele, A. Cosijns, I. De Paepe, P.J.S. Jacobs, L. Van Hoorebeke, J.P. Remon, E. Schacht, Porous Gelatin Hydrogels: 1, Cryogenic Formation and Structure Analysis, Biomacromolecules 8 (2) (2007) 331–337.
[36] Q. Liu, W.-Q. He, M. Aguedo, X. Xia, W.-B. Bai, Y.-Y. Dong, J.-Q. Song, A. Richel, D. Goffin, Microwave-assisted alkali hydrolysis for cellulose isolation from wheat straw: Influence of reaction conditions and non-thermal effects of microwave, Carbohydr. Polym. 253 (2021), 117170.
[37] Y. Wang, X. Chen, Y. Kuang, M. Xiao, Y. Su, F. Jiang, Microstructure and filtration performance of konjac glucomannan-based aerogels strengthened by wheat straw, International Journal of Low-Carbon Technologies 13 (1) (2018) 67–75.
[38] F.T. Jiang, A sound-absorbing and noise-reducing plant polysaccharide-based aerogel and preparation method [(Pattern NO: 108285556 A). CN].
[39] X. Ni, F. Ke, M. Xiao, K. Wu, Y. Kuang, H. Corke, F. Jiang, The control of ice crystal growth and effect on porous structure of konjac glucomannan-based aerogels, Int. J. Biol. Macromol. 92 (2016) 1130–1135.
[40] J. Babaei, M. Mohammadian, A. Madadlou, Gelatin as texture modifier and porogen in egg white hydrogel, Food Chem. 270 (2019) 189–195.
[41] H. Jin, Y. Nishiyama, M. Wada, S. Kuga, Nanofibrillar cellulose aerogels, Colloids Surf., A 240 (1–3) (2004) 63–67.
[42] H. Kiani, D.-W. Sun, Water crystallization and its importance to freezing of foods: A review, Trends Food Sci. Technol. 22 (8) (2011) 407–426.
[43] Y. Wang, Y. Su, W. Wang, Y. Fang, S.B. Riffat, F. Jiang, The advances of polysaccharide-based aerogels: Preparation and potential application, Carbohydr. Polym. 226 (2019), 115242.
[44] H. Qui, Y. Enhui, Effect of thickness, density and cavity depth on the sound absorption properties of wool boards, Autex Research Journal 18 (2) (2018) 203–208.
[45] R. Dunne, D. Desai, R. Sadiku, A review of the factors that influence sound absorption and the available empirical models for fibrous materials, Acoustics Australia 45 (2) (2017) 453–469.
[46] Z. Li, L. Zhang, C. Mao, Z. Song, X. Li, C. Liu, Preparation and characterization of konjac glucomannan and gum arabic composite gel, Int. J. Biol. Macromol. 183 (2021) 2121–2130.
[47] D. Qiao, Z. Wang, C. Cai, S. Yin, H. Qian, B. Zhang, F. Jiang, X. Fei, Tailoring Multi-Level Structural and Practical Features of Gelatin Films by Varying Konjac Glucomannan Content and Drying Temperature, Polymers 12 (2) (2020) 385.
[48] S.H. Ghaffar, M. Fan, Revealing the morphology and chemical distribution of nodes in wheat straw, Biomass Bioenergy 77 (2015) 123–134.
[49] L. Shen, H. Zhang, Y. Lei, Y. Chen, M. Liang, H. Zou, Hierarchical pore structure based on cellulose nanofiber/melamine composite foam with enhanced sound absorption performance, Carbohydr. Polym. 255 (2021), 117405.
[50] R.S. Rivlin, D.W. Saunders, E.N.D.C. Andrade, Large elastic deformations of isotropic materials VII. Experiments on the deformation of rubber, Philos. Trans. R. Soc. London Ser. A, Math. Phys. Sci. 243 (865) (1951) 251–288.
[51] R.W. Ogden, R. Hill, Large deformation isotropic elasticity – on the correlation of theory and experiment for incompressible rubberlike solids, Proceedings of the Royal Society of London. A. Mathematical and Physical Sciences 326(1567) (1972) 565-584.
[52] O.H. Yeoh, Some Forms of the Strain Energy Function for Rubber, Rubber Chem. Technol. 66 (5) (1993) 754–771.
[53] L.R.G. Treloar, The elasticity and related properties of rubbers, Rep. Prog. Phys. 36 (7) (1973) 755–826.